Reduced Energy Expenditure and Increased Inflammation Are Early Events in the Development of Ovariectomy-Induced Obesity

Nicole H. Rogers, James W. Perfield II, Katherine J. Strissel, Martin S. Obin, and Andrew S. Greenberg

Obesity and Metabolism, Jean Mayer United States Department of Agriculture Human Nutrition Research Center on Aging at Tufts University, Boston, Massachusetts 02111

Menopause, an age-related loss of ovarian hormone production, promotes increased adiposity and insulin resistance. However, the diet-independent mechanism by which loss of ovarian function promotes increased adipose tissue mass and associated metabolic pathologies remains unclear. To address this question, we monitored food intake and weight gain of ovariectomized (OVX) mice and sham OVX (SHM) mice for 12 wk. Although food intake was similar, OVX mice gained 25% more weight than SHM mice. Moreover, the OVX mice accumulated 4.7- and 4.4-fold more perigonadal and inguinal adipose tissue by weight, respectively, with 4.4-fold (perigonadal, $P < 0.001$) and 5.3-fold (inguinal, $P < 0.01$) larger adipocytes and no change in adipocyte cell number. OVX-induced adiposity was coincident with an 18% decrease in metabolic rate during the dark phase ($P = 0.001$) as well as an 11% decrease during the light phase ($P = 0.03$). In addition, ambulatory activity levels of OVX mice were decreased only during the dark phase (40%, $P = 0.008$). OVX mice displayed evidence of immune infiltration and inflammation in adipose tissue, because perigonadal and inguinal adipose depots from OVX mice had increased expression of TNFα, iNOS, CD11c, and other hallmarks of adipose tissue inflammation. In contrast, expression of the T cell marker CD3 (3.5-fold, $P = 0.03$) and Th1 cytokine interferon-γ (IFNγ) (2.6-fold, $P = 0.02$) were elevated in perigonadal but not sc fat. Finally, histology revealed OVX-specific liver hepatic steatosis, coincident with increased PPARγ gene expression and downstream lipogenic gene expression. In summary, OVX in mice decreases energy expenditure, without altering energy intake, resulting in adipocyte hypertrophy, adipose tissue inflammation, and hepatic steatosis. (***Endocrinology*** **150: 2161–2168, 2009)**

Menopause, the age-related loss of ovarian hormone production, is associated with increased visceral adiposity and related metabolic pathologies including insulin resistance, type 2 diabetes, and cardiovascular disease (1–4). The personal and public health impacts of menopause-associated disease are significant, because women can now expect to spend nearly a third of their lives in the menopausal state. These observations highlight the importance of understanding the molecular and physiological mechanisms that underlie menopause-associated obesity and metabolic dysregulation. Currently, however, these mechanisms remain unclear.

Rodent ovariectomy (OVX) is one approach to modeling human menopause and studying the metabolic consequences of loss of ovarian function. Studies in rodents consistently demonstrate that OVX promotes obesity and its metabolic complications, in particular insulin resistance. However, these studies have been in large part confounded by OVX-induced hyperphagia (5–8), which makes it difficult to distinguish the effects of OVX on obesity and insulin resistance independently from the effects of overnutrition. Using a pair-feeding paradigm, we recently reported that estrogen repletion of OVX mice prevented gains in adiposity independent of food intake (9), suggesting that altered metabolic rate may be contributing to the obese phenotype in OVX mice. Recent studies suggest that decreased energy expenditure contributes to the increase in visceral adiposity in menopausal women (10). However, the diet-independent mechanisms by which

ISSN Print 0013-7227 ISSN Online 1945-7170
Printed in U.S.A.

doi: 10.1210/en.2008-1405 Received October 3, 2008. Accepted January 16, 2009.
First Published Online January 29, 2009

Abbreviations: ACC-1, Acetyl-coenzyme A carboxylase-1; AT, adipose tissue; BW, body weight; CLS, crown-like structure; DC, dendritic cell; FAS, fatty acid synthase; IFNγ, interferon-γ; iNOS, inducible nitric oxide synthase; MΦ, macrophage; MCP-1, monocyte chemoattractant protein-1; OVX, ovariectomy; PGAT, perigonadal adipose tissue; PPARγ, peroxisome proliferator-activated receptor-γ; RANTES, regulated on activation normal T expressed and secreted; SCAT, sc adipose tissue; SHM, sham OVX; Th1, T-helper 1.

loss of ovarian function promotes increased adipose tissue (AT) mass and insulin resistance remain largely undetermined.

Obesity, and in particular visceral adiposity, is associated with chronic AT inflammation, which is now implicated as an underlying cause of obesity-associated metabolic pathology in humans and rodents (reviewed in Refs. 11 and 12). Infiltration of AT by immune cells appears to play a central role in the etiology of AT inflammation and its pathological sequelae (13–15). A hallmark feature of AT inflammation in mice is the recruitment and accumulation of proinflammatory AT macrophages (MΦs) expressing the dendritic cell (DC) marker CD11c (13, 14, 16). These MΦs are recruited by chemokines, such as monocyte chemoattractant protein-1 (MCP-1 or CCL2) and osteopontin, and secrete TNFα, IL-6, nitric oxide (NO), and additional inflammatory, atherogenic and procoagulant mediators that are implicated in the development of insulin resistance and vascular complications of obesity (17, 18). More recently, T cell infiltration has been reported in chronically obese mice (15), and upregulated expression of the T helper 1 (Th1) cytokine interferon-γ (IFNγ) has been associated with obesity (19). Intriguingly, estrogen has anti-inflammatory and vasoprotective properties (20), suggesting that loss of ovarian function could further promote such complications. Currently, the effects of OVX on AT inflammation are entirely unknown.

The present study investigates proximate mechanisms of increased adiposity and AT inflammation during the development of OVX-induced obesity and insulin resistance. Employing a mouse model in which food intake does not increase as a consequence of loss of ovarian function, we identify reduced metabolic expenditure as an early mechanism underlying OVX-induced increases in adiposity (and associated insulin resistance). In addition, we provide the first evidence supporting a role for T cells and $CD11c^+$ MΦs in OVX-associated AT inflammation, and we identify distinct depot-dependent inflammatory profiles that are consistent with the inordinate contribution of visceral AT to the development of metabolic complications in postmenopausal women (21).

Materials and Methods

Animals

Sham-OVX (SHM) and OVX C57B/6J mice were purchased from Charles River Laboratories (Wilmington, MA), with operations performed at 10 wk of age. All animals were housed in an Association for the Assessment and Accreditation of Laboratory Animal Care (AAALAC)-approved animal facility with 12-h light, 12-h dark cycles and given free access to water and food (phytoestrogen-free chow; Harlan Teklad, Madison, WI). Mice were individually housed, food intake was monitored daily, and body weight (BW) was monitored biweekly. After 12 wk, mice were fasted for 8 h and killed by cervical dislocation. Blood was taken by cardiac puncture, and tissues were immediately harvested.

Plasma analyses

Blood glucose was measured with an automated glucometer (One touch Ultra; LifeScan, Inc., Milpitas, CA), plasma insulin was determined using an ELISA with mouse insulin as a standard (Crystal Chem, Downers Grove, IL), plasma estradiol levels were determined using an ELISA (Cayman Chemical, San Diego, CA), and plasma triglycerides and nonesterified fatty acid levels were determined using commercial kits (Wako Chemicals, Richmond, VA).

Indirect calorimetry

At 9–10 wk after operation, subsets of mice (n = 7 per group) were placed in metabolic chambers (TSE Calorimetry Systems, Chesterfield, MO) for 3 d with free access to food and water. This system is designed to simultaneously and continuously monitor O_2 consumption, CO_2 production, and ambulatory movement using a photobeam break system. Data were collected every 3 min for 72 h, with the first 24 h considered an acclimatization period and excluded from analyses. Oxygen consumption was calculated per gram of metabolic BW, or $(BW)^{0.75}$.

Histology

Using a subset of mice (n = 4 per group), small pieces of dissected perigonadal AT (PGAT), inguinal sc AT (SCAT), and liver were fixed in 4% formaldehyde, embedded in paraffin, sectioned, and stained with hematoxylin and eosin. Digital images were acquired with an Olympus DX51 light microscope.

Immunohistochemistry

Histological sections of PGAT were dewaxed in xylenes, rehydrated through an ethanol series, and stained using avidin-biotin kits for TNFα (Epitomics Inc., Burlingame, CA) and F4/80 (Vector Laboratories, Burlingame, CA) following manufacturer's instructions. Antibodies used were rabbit antimouse TNFα (Abcam, Cambridge, MA), and rat antimouse F4/80 (Serotec, Raleigh, NC). Sections were then counterstained with hematoxylin. Tissue from TNFα knockout mice and nonimmune IgG (rat) were used as negative controls.

Cell size and number

Adipocyte volume (mean ± SEM) was calculated from adipocyte cross-sectional area obtained from perimeter tracings of adipocytes on digital images of histological sections using a graphics tablet pen and Image J software (Sun Microsystems, Palo Alto, CA). For each mouse, tracings were obtained from more than 100 adipocytes in each of three separate sections. Adipocyte number was calculated from fat pad weight and adipocyte volume as described (22).

RNA isolation, RT, and real-time quantitative PCR

Dissected tissues (with lymph nodes removed) were immediately snap-frozen in liquid nitrogen and stored at −80 C. AT RNA was extracted using QIAGEN Lipid Mini kits (Valencia, CA), and liver RNA was isolated using QIAGEN Mini kits according to manufacturer's instructions. RNA was quantified and checked for purity using the Nanodrop spectrophotometer (Nanodrop 1000, Wilmington, DE). First-strand cDNA was generated from 1 μg RNA using AMV Reverse Transcriptase (Promega, Madison, WI), and real-time quantitative PCR was performed using SYBR Green technology (Applied Biosystems 7300, Foster City, CA). Fold changes were calculated as $2^{-\Delta\Delta CT}$ with the average of 36B4 and cyclophilin B used as the endogenous control for AT and the average of the endogenous control genes 36B4 and 18S used for liver. Primer sequences are available upon request.

Statistical analyses

All data are presented as means ± SEM. Treatment effects were assessed for statistical significance ($P \leq 0.05$) by Student's *t* tests (Excel) or ANOVA followed by Tukey's procedure for *post hoc* pair-wise comparisons (Systat version 10).

Results

Body weight, uterine weight, and fasting plasma profiles

As confirmation of successful OVX-induced suppression of endogenous estrogen production, OVX uterine weight was sig-

TABLE 1. Physiological measurements of female SHM and OVX mice 12 wk after operation

Variable	SHM	OVX
BW (g)	22.8 ± 0.1	27.5 ± 0.1[a]
Uterine weight (g)	0.081 ± 0.008	0.040 ± 0.008[a]
Plasma estradiol (pmol/liter)	305.9 ± 176	12.3 ± 6[a]
Glucose (mmol/liter)	5.8 ± 0.26	7.4 ± 0.42[a]
Insulin (pmol/liter)	145.3 ± 23.4	207.8 ± 47.4
Triglycerides (mmol/liter)	0.34 ± 0.04	0.34 ± 0.03
NEFA (mmol/liter)	0.66 ± 0.17	0.49 ± 0.10

Plasma measures of glucose, insulin, and triglycerides were determined after an 8-h fast. NEFA, Nonesterified fatty acids. n ≥ 7.

[a] $P \leq 0.05$.

nificantly decreased compared with SHM mice. At 12 wk after operation, OVX mice weighed 27.50 ± 0.10 g, whereas the SHM mice weighed significantly less at only 22.76 ± 0.11 g. Fasting plasma glucose levels were significantly elevated in the OVX mice (7.4 ± 0.42 mmol/liter *vs.* SHM 5.8 ± 0.26 mmol/liter, $P < 0.001$). Average fasting insulin, triglyceride, and nonesterified free fatty acids levels were not significantly different between the groups. These data suggest that OVX mice compared with SHM mice had alterations in glucose/insulin homeostasis. SHM and OVX mice uterine weight, BW, and fasting plasma nutrient and hormone levels are depicted in Table 1.

Energy intake, energy expenditure, and ambulatory activity

Previous studies in rats have indicated that OVX induces hyperphagia (5–8). In contrast, we found no significant differences in daily food intake, shown as weekly averages in Fig. 1A, with the exception of wk 8 when OVX mice actually consumed less than SHM mice. Importantly, this model gave us the opportunity to study OVX-induced metabolic dysregulation that is independent of food intake, something many previous rodent studies have not done. We found that despite eating similar amounts of food, OVX mice gained significantly more weight than SHM mice over the course of 12 wk (Fig. 1B). More specifically, the OVX mice gained almost twice as much BW per kilojoule consumed (Fig. 1C), indicating an increased propensity to store energy as BW, or elevated feeding efficiency. Therefore, we used indirect calorimetry to calculate energy expenditure. OVX mice consumed significantly less oxygen than SHM mice, during both the dark and light phases (Fig. 2A). Spontaneous physical activity levels during the dark phase were significantly lower in the OVX group, but there were no differences in the light phase (Fig. 2B). Together, these results demonstrate that loss of ovarian function in mice decreases 24-h energy expenditure and promotes less ambulatory activity during the dark phase without altering energy intake.

AT expansion

After normalizing for total BW, PGAT (4.7-fold, $P < 0.001$) and SCAT (4.4-fold, $P < 0.001$) depot weights were significantly increased in the OVX mice compared with SHM (Fig. 3A). OVX mice tended to store more fat in PGAT as compared with SCAT; in contrast, body fat was more equally distributed between the

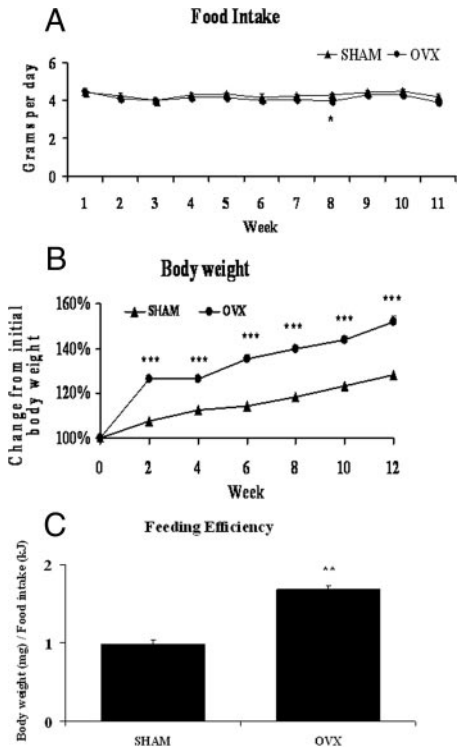

FIG. 1. OVX mice gain more weight despite similar food intake. Average daily food intake (A) and weight gain expressed as a percentage of starting weight (B) were determined for SHAM (*triangles*) and OVX (*circles*) mice. Feeding efficiency was calculated as milligrams of BW gained per kilojoule of energy consumed (C). *Error bars* indicate SEM. n = 22. *, $P < 0.05$; **, $P < 0.01$; ***, $P < 0.001$.

two depots in SHM (treatment × depot interaction: trend, $P = 0.08$) (Fig. 3A). Adipocyte volume was 4.4-fold greater in PGAT ($P < 0.001$) and 5.3-fold greater in SCAT ($P < 0.01$) of OVX mice (Fig. 3B). In addition, when adipocyte number was calculated, there were no significant differences between SHM and OVX mice in either depot (data not shown), indicating that the increased AT weight in OVX mice reflects adipocyte hypertrophy.

AT inflammatory state

We next used the ΔΔCt method of real-time PCR to determine the relative mRNA expression of immune cell markers, chemokines, and inflammatory cytokines (relative to the endogenous control genes cyclophilin B and 36B4) in PG and SCAT from SHM and OVX mice. We found that expression of the T cell marker CD3 was significantly up-regulated (3.7-fold, $P = 0.03$) in PGAT from OVX mice relative to SHM mice, strongly suggesting T cell infiltration (Fig. 4A). MΦ markers F4/80 and CD11b were up-regulated 1.7- and 2.3-fold, respectively, and the DC marker CD11c was elevated more than 6-fold (Fig. 4A) compared with SHM mice. These results are consistent with the preferential infiltration of $CD11c^+$ ATMΦs into PGAT of OVX mice. T cell and DC recruitment to PGAT was coincident with up-regulated expression of the lymphokine regulated on activation normal T expressed and secreted (RANTES or CCL5), the chemokines MCP-1 (3.2-fold) and osteopontin (2-fold), as well as induction of the proinflammatory cytokines IFNγ (2.4-fold), TNFα (3.6-fold), IL-1β (4.2-fold), and IL-6 (7.5-fold) (Fig. 4A).

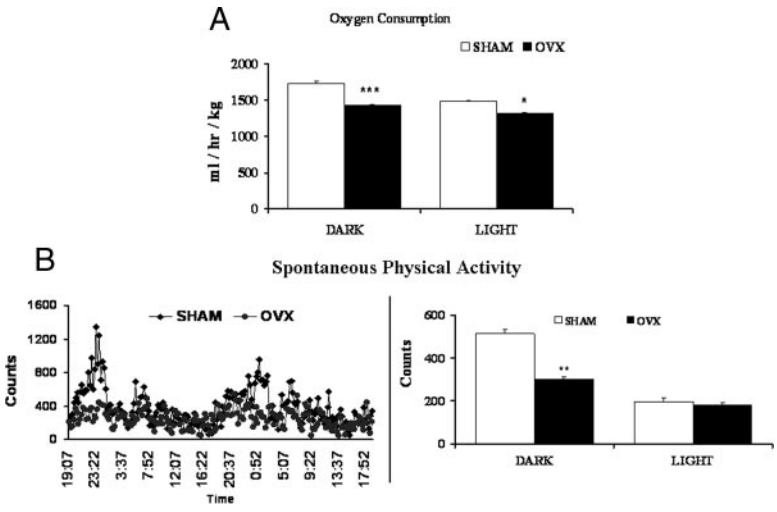

FIG. 2. OVX mice have decreased oxygen consumption and ambulatory activity levels. TSE calorimeters were used to measure 48-h average oxygen consumption (A) and spontaneous physical activity (B) of SHAM (*white bars*) and OVX (*black bars*) mice during the dark phase (1900–0700 h) and the light phase (0700–1900 h). Consumption is normalized for metabolic BW [(BW in kilograms) $^{0.75}$]. *Error bars* indicate SEM. n = 7. *, $P < 0.05$; **, $P < 0.01$; ***, $P < 0.001$.

Inducible nitric oxide synthase (iNOS) mRNA was also increased 2.1-fold, coincident with a 75% reduction in arginase expression, a negative regulator of NO production and a marker of alternative (M2) MΦ activation (23).

Analysis of representative histological sections of PGAT revealed MΦs arranged in visible crown-like structures (CLSs), consistent with MΦs engulfing dead adipocytes (24) in all OVX mice examined (four of four), whereas no CLSs were visible in PGAT of SHM mice (zero of four, data not shown). Further immunohistochemical studies on adjacent sections of PGAT from OVX and SHM mice demonstrated that CLS-associated ATMÔs (F4/80$^+$ cells) were synthesizing readily detectable levels of TNFα protein (Fig. 4C).

The gene expression profile of OVX-induced inflammatory changes in SCAT was distinct from that observed in PGAT (compare Fig. 4, B with A). Most notably, we detected no increase in CD3 gene expression (Fig. 4B), suggesting that T cell infiltration is not a feature of SCAT in the early development of OVX-induced obesity. Additionally, in contrast to PGAT, we detected no induction of IFNγ gene expression, and we detected an actual down-regulation of RANTES in SCAT (Fig. 4*B*). This down-regulation appeared to be specific for RANTES, because the chemokines MCP-1 and osteopontin were significantly up-regulated in SCAT in response to OVX (Fig. 4B). Osteopontin gene up-regulation was in fact greater in SCAT (4.6-fold) than in PGAT (treatment × depot interaction, $P = 0.05$). Up-regulated F4/80 (1.7-fold), CD11b (3.1-fold), and CD11c (3-fold) gene expression in SCAT indicate the recruitment of CD11c$^+$ MΦs (Fig. 4*B*). However, the magnitude of CD11c expression in SCAT was significantly less than that measured in PGAT (Fig. 4A, treatment × depot interaction, $P = 0.01$), suggesting that in response to OVX, recruitment of CD11c$^+$ ATMΦs is less robust in SCAT as compared with PGAT (see *Discussion*).

In notable contrast to PGAT, neither IL-1B nor IL-6 genes were significantly up-regulated in SCAT in response to OVX (Fig. 4B). The effect of OVX on expression of the M2 markers IL-10 and arginase was essentially identical in SCAT as compared with PGAT. Together these results suggest that OVX-induced AT inflammation is more severe in PGAT than in SCAT.

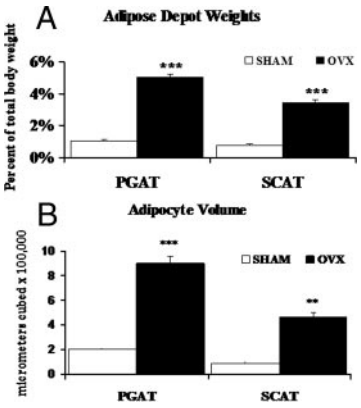

FIG. 3. OVX mice display evidence of increased AT weight and adipocyte hypertrophy. PGAT and SCAT depots were weighed and normalized for total BW (A), and average adipocyte cell volume (B) was calculated for SHM (*white bars*) and OVX (*black bars*) mice. *Error bars* indicate SEM. n = 4–6. **, $P < 0.01$; ***, $P < 0.001$.

Liver lipogenesis and inflammation

Adipose tissue inflammation and MΦ infiltration are correlated with increased fat deposition in liver (25), a pathology that is itself associated with the development of insulin resistance, independent of adiposity (26). Therefore, we examined livers from SHM and OVX mice for evidence of hepatic steatosis. Histological analyses revealed enlarged lipid droplets in livers from OVX mice, compared with SHM (Fig. 5A). Expression of the transcription factor peroxisome proliferator-activated receptor-γ (PPARγ) was elevated over 10-fold ($P = 0.002$), and mRNA levels of the downstream lipogenic genes fatty acid synthase (FAS) and acetyl-coenzyme A carboxylase-1 (ACC-1) were increased 2.5-fold ($P = 0.02$) and 1.6-fold ($P = 0.05$), respectively (Fig. 5B). Steatotic livers of OVX mice also displayed evidence of inflammation, because TNFα (1.8-fold, $P < 0.001$), osteopontin (1.9-fold, $P = 0.03$), and MCP-1 (1.8-fold, $P = 0.01$) gene expression were elevated (Fig. 5B).

Discussion

Human menopause is associated with increased visceral adiposity and elevated risk of metabolic disease, but molecular mechanisms remain unclear. Rodent OVX is one approach to model human menopause and study the effects of loss of ovarian function. Prior studies in rodents have shown that OVX increases adiposity and insulin resistance, but these studies have primarily been performed in rats, which become hyperphagic (5–8), thereby confounding metabolic studies. We have previously shown that estrogen repletion of OVX mice decreases AT mass

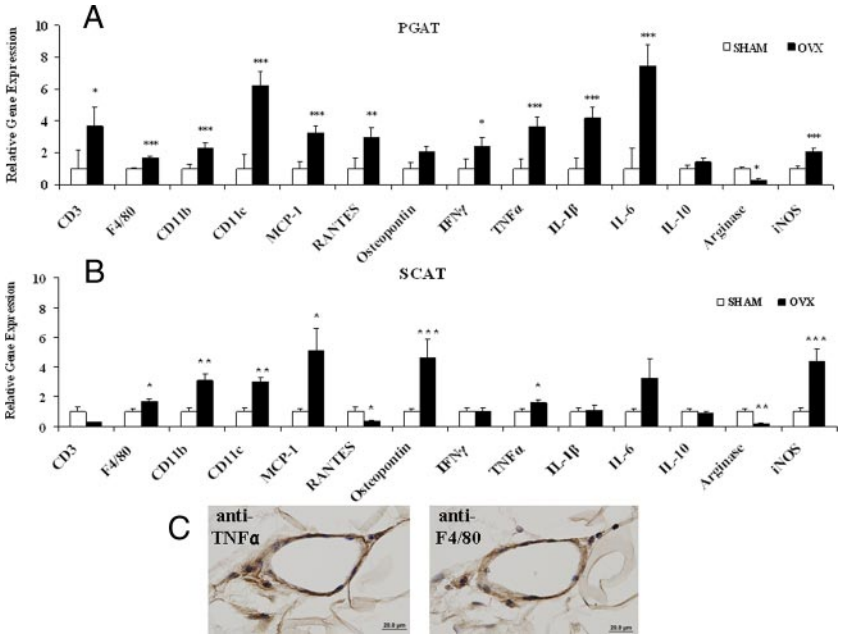

FIG. 4. OVX mice have increased AT inflammation. Quantitative real-time PCR (relative to the endogenous target genes cyclophilin B and 36B4) was performed to determine the expression of inflammatory mediators in PGAT (A) and inguinal SCAT (B) harvested from SHM (*white bars*) and OVX (*black bars*) mice. *Error bars* indicate SEM. n = 7–10. *, $P < 0.05$; **, $P < 0.01$; ***, $P < 0.001$. C, Representative histochemical staining of adjacent sections of PGAT from OVX mice using anti-TNFα (*left panel*, *brown stain*) or anti-F4/80 (*right panel*, *brown stain*) demonstrates that F4/80$^+$ cells (MΦs) within CLSs synthesize TNFα.

compared with pair-fed OVX mice (9). We now expand those findings to a mouse model of menopause where OVX and SHM mice ate *ad libitum* but consumed equivalent amounts of food. We demonstrate that compared with SHM, OVX mice display decreased energy expenditure, resulting in dramatic adipocyte hypertrophy and PGAT and SCAT expansion.

While this manuscript was in preparation, another study was published confirming that OVX mice do not become hyperphagic and display decreased energy expenditure after 24 wk (27). Importantly, the decrease in energy expenditure seen in the OVX mice is potentially relevant to humans because postmenopausal women display marked decreases in energy expenditure without increases in food intake (10). However, it is important to note that in comparison with humans, rodent brown AT is thought to have a more significant role in energy metabolism and could be contributing to the observed changes in overall metabolic rate observed in this mouse model of menopause.

Analysis of spontaneous activity levels indicated that the decrease in energy expenditure seen in OVX mice in the dark phase is associated with lower ambulatory activity. Decreased activity with loss of ovarian function is consistent with studies of ERα knockout mice (28) and OVX rats (29). It is noteworthy, however, that there was still a decrease in oxygen consumption during the light phase, a time when the mice are presumably sleeping, and there were no differences in activity levels, suggesting that OVX decreases energy expenditure via both activity-dependent and independent mechanisms. This is again consistent with human data demonstrating menopause-associated decreases in free-living energy expenditure, 24-h energy expenditure, and activity levels, as well as sleeping energy expenditure (10).

To gain further insight into the metabolic pathology associated with loss of ovarian function in mice, we investigated inflammatory changes occurring in AT of SHM and OVX mice, because the infiltration and proinflammatory activation of immune cells in AT is now recognized as an underlying cause of obesity complications (7–9). The present study provides, to our knowledge, the initial characterization of AT inflammation in a mouse model of menopause. A strength of our data are the absence of potentially confounding effects of either overnutrition (*e.g.* hyperphagia) or high-fat feeding, both of which can activate the innate immune system independent of adiposity (13, 30). Our data indicate that OVX-associated increases in adiposity and insulin resistance (elevated fasting blood glucose levels) are coincident with the up-regulation of monocytic cell chemoattractants (MCP-1, osteopontin, and RANTES), the accumulation of proinflammatory ATMΦs (*e.g.* F4/80$^+$/CD11b$^+$/CD11c$^+$ cells), and the up-regulation of proinflammatory mediators (TNF-α, IL-1β, IL-6, and NO) implicated in the development of insulin resistance (31, 32). Moreover, immunohistochemistry indicated that MΦs arranged in CLSs are at least one source of the excess TNFα being produced in perigonadal AT from OVX mice.

Concomitant with these proinflammatory changes, we noted down-regulation of arginase, a marker of M2 (alternative) MΦ polarization. This proinflammatory profile is highly similar to the phenotypic switch of ATMΦs toward M1 (classic) polarization that is coincident with the development of insulin resistance in obese insulin-resistant male mice. We and others have demonstrated that a hallmark of this phenotypic switch is the accumula-

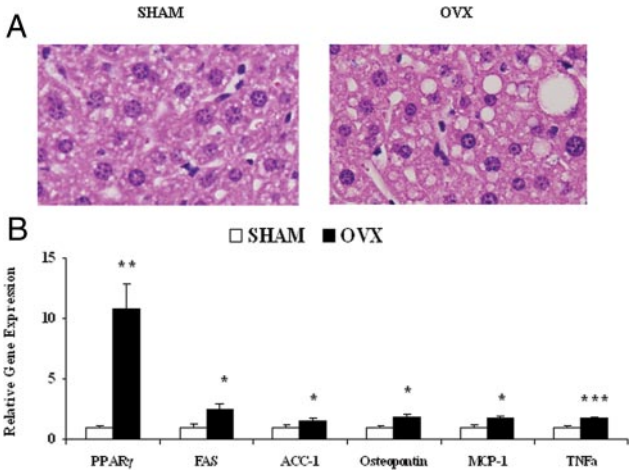

FIG. 5. OVX mice display early hepatic steatosis and inflammation. A, Representative hematoxylin and eosin staining demonstrates more lipid droplet development in liver sections from OVX mice. B, Liver gene expression determined using quantitative real-time PCR (relative to the average of the endogenous genes 18S and 36B4). *Error bars* indicate SEM. n = 7–10. *, $P < 0.05$; **, $P < 0.01$; ***, $P < 0.001$.

tion of F4/80$^+$/CD11b$^+$/CD11c$^+$ ATMΦs that express high levels of TNFα, iNOS, and other inflammatory mediators (13, 14). Notably, abrogation of CD11c$^+$ ATMs protects against the development of obesity-associated insulin resistance in male mice (33). Our data strongly suggest that a similar phenotypic switch in ATM populations and polarization occurs in response to OVX.

Intriguingly, in contrast to AT of male mice made obese by a high-fat diet (13), AT of OVX mice did not up-regulate gene expression of IL-10, an inflammation-suppressive cytokine that protects adipocytes from the deleterious effects of TNFα (14). Because IL-10 gene expression can be induced by lipopolysaccharide (34), this difference may reflect the induction of IL-10 in male mice by high-fat diet-induced endotoxemia (13).

In addition to alterations in ATMΦ phenotype, OVX was associated with elevated expression of the T cell marker CD3, the Th1 cytokine IFNγ, and the lymphokine RANTES (CCL5) in PGAT (but not in SCAT). T-helper cells play a critical role in orchestrating immune response by modulating and coordinating the local inflammatory responses of antigen-presenting cells such as MΦs and DCs. In the traditionally dichotomous Th1/Th2 paradigm, local secretion of IFNγ by Th1 cells activates classical proinflammatory responses of MΦs and DCs, including up-regulation of M1 cytokines such as TNFα and IL-1β. Rocha *et al.* (15) recently reported that Th1 lymphocytes regulate inflammatory responses in AT of obese male mice and demonstrated a role for IFNγ production in inflammation-driven insulin resistance. Indeed, in the present study, gene expression of MΦ markers F4/80 and CD11b was comparable in PGAT and SCAT after OVX, but CD11c$^+$ gene expression was significantly greater in PGAT. This result suggests that M1 polarization of ATMΦs is more robust in PGAT as compared with SCAT of OVX mice. In support of this notion, gene expression of M1 cytokines (*e.g.* TNFα, IL-1β, andIL-6) was also significantly greater in PGAT as compared with SCAT. Because Th1 activity contributes to M1 polarization, we propose that the attenuated M1 polarization state of ATMΦs in SCAT reflects the relative absence of Th1 recruitment and Th1 cytokine (IFNγ) expression. A caveat of our study is that we measured cytokine gene expression in whole AT and thus cannot distinguish cytokine production by ATMΦs from cytokine production by other AT cells.

Visceral AT mass is directly associated with increased inflammatory cytokine production and metabolic dysfunction (13). Recent human data demonstrate that visceral AT contributes to the metabolic complications of menopause (35). In the current paper, we demonstrate that OVX results in a greater inflammatory tone in visceral AT, characterized by infiltration and proinflammatory activation of and CD11c$^+$ ATMΦs and T cells and speculate similar alterations may in part explain the metabolic complications associated with menopause.

T cell involvement in OVX-associated bone loss is well documented, because studies have demonstrated that the increase in bone TNFα in OVX mice reflects TNFα gene expression in T lymphocytes (reviewed in Ref. 36). Moreover, these reports implicate IFNγ production as a mediator of inflammatory actions on bone that are observed in the absence of ovarian hormones. Here, we have expanded these observations by suggesting that lymphocytes and IFNγ production also play important roles in OVX-associated AT inflammation.

Obesity and AT inflammation are highly associated with a variety of metabolic pathologies (37), including liver steatosis and nonalcoholic steatohepatitis (25). A number of murine models with hepatic steatosis display elevated levels of PPARγ in liver (38–42). Consistent with a role for PPARγ in facilitating hepatic lipid deposition, liver-specific delivery of PPARγ *in vivo*, using a viral vector, results in hepatic steatosis (43). In the present study, livers from OVX mice displayed visible steatosis that was coincident with a remarkable 10-fold elevation in hepatic PPARγ expression. PPARγ overexpression in hepatocytes turns on a program increasing lipogenic gene expression (44). Indeed, we observed higher expression of two genes involved in lipogenesis, FAS and ACC-1, in livers from OVX mice. Consistent with our observations, administration of estrogen to genetically obese (*ob/ob*) mice down-regulates expression of FAS and ACC-1 in liver and decreases hepatic triglyceride levels (45). In light of these observations, our results strongly suggest that a mechanism by which OVX mice develop hepatic steatosis is via up-regulation of PPARγ.

As reported in studies of diet-induced nonalcoholic steatohepatitis (46), OVX-induced hepatic steatosis in the present study was associated with induction of hepatic TNFα and osteopontin expression. The latter is a Th1 cytokine implicated in the progressive pathophysiology of hepatic inflammation and cancer (37, 38) as well as the development of insulin resistance (47) and atherosclerosis (48). Our results demonstrate that loss of ovarian function in mice promotes osteopontin production in both AT and liver, making these tissues potentially important contributors to the elevated circulating levels of osteopontin previously reported in OVX rodents (49).

We conclude that OVX in mature female mice is associated with decreased energy expenditure, AT expansion, and hepatic steatosis. We are the first, to our knowledge, to identify distinct depot-dependent inflammatory profiles that support a role for T cells and CD11c$^+$ MΦs in OVX-associated AT inflammation, highlighting the loss of ovarian function as a metabolic risk factor that can promote a deleterious state of chronic inflammation, even in the absence of dietary changes. These data provide one potential explanation for the increased susceptibility to metabolic diseases observed with menopause and suggest future clinical studies should investigate menopause-associated changes in AT cell populations and cytokine production. Moreover, these data suggest that OVX mice will display a compromised homeostatic response to a metabolic challenge, such as high-fat diet, that predisposes to the development of obesity and insulin resistance. If confirmed in human studies, these observations would be clinically relevant to the growing menopausal population in a society defined by energy overconsumption. Future studies will address these predictions.

Acknowledgments

We thank Dr. Richard Karas and Dr. Jennifer Sacheck for their thoughtful insight during manuscript preparation and Tufts Comparative Biology Unit for excellent animal care.

Address all correspondence and requests for reprints to: Andrew S. Greenberg, M.D., Jean Mayer United States Department of Agriculture Human Nutrition Research Center on Aging at Tufts University, Obesity and Metabolism Room 608, Boston, Massachusetts 02111. E-mail: Andrew.greenberg@tufts.edu, martin.obin@tufts.edu.

This work was supported by U.S. Department of Agriculture Grant 5819507707 and National Institutes of Health Grants T32DK062032, DK-50647, and DK074979 and Grant W81XWH-07-1-0597. A.S.G. is a recipient of an endowed chair from the Robert C. and Veronica Atkins Foundation.

Disclosure Summary: The authors have nothing to disclose.

References

1. **Carr DB, Utzschneider KM, Hull RL, Kodama K, Retzlaff BM, Brunzell JD, Shofer JB, Fish BE, Knopp RH, Kahn SE** 2004 Intra-abdominal fat is a major determinant of the National Cholesterol Education Program Adult Treatment Panel III criteria for the metabolic syndrome. Diabetes 53:2087–2094
2. **Ferrara CM, Lynch NA, Nicklas BJ, Ryan AS, Berman DM** 2002 Differences in adipose tissue metabolism between postmenopausal and perimenopausal women. J Clin Endocrinol Metab 87:4166–4170
3. **Tchernof A, Despres JP** 2000 Sex steroid hormones, sex hormone-binding globulin, and obesity in men and women. Hormone Metab Res 32:526–536
4. **dos Reis CM, de Melo NR, Meirelles ES, Vezozzo DP, Halpern A** 2003 Body composition, visceral fat distribution and fat oxidation in postmenopausal women using oral or transdermal oestrogen. Maturitas 46:59–68
5. **Meli R, Pacilio M, Raso GM, Esposito E, Coppola A, Nasti A, Di Carlo C, Nappi C, Di Carlo R** 2004 Estrogen and raloxifene modulate leptin and its receptor in hypothalamus and adipose tissue from ovariectomized rats. Endocrinology 145:3115–3121
6. **Liang YQ, Akishita M, Kim S, Ako J, Hashimoto M, Iijima K, Ohike Y, Watanabe T, Sudoh N, Toba K, Yoshizumi M, Ouchi Y** 2002 Estrogen receptor β is involved in the anorectic action of estrogen. Int J Obes Relat Metab Disord 26:1103–1109
7. **Wade GN, Gray JM** 1979 Gonadal effects on food intake and adiposity: a metabolic hypothesis. Physiol Behav 22:583–593
8. **Richard D** 1986 Effects of ovarian hormones on energy balance and brown adipose tissue thermogenesis. Am J Physiol 250:R245–R249
9. **D'Eon TM, Souza SC, Aronovitz M, Obin MS, Fried SK, Greenberg AS** 2005 Estrogen regulation of adiposity and fuel partitioning. Evidence of genomic and non-genomic regulation of lipogenic and oxidative pathways. J Biol Chem 280:35983–35991
10. **Lovejoy JC, Champagne CM, de Jonge L, Xie H, Smith SR** 2008 Increased visceral fat and decreased energy expenditure during the menopausal transition. Int J Obes 32:949–958
11. **Hotamisligil GS** 2006 Inflammation and metabolic disorders. Nature 444:860–867
12. **Greenberg AS, Obin MS** 2006 Obesity and the role of adipose tissue in inflammation and metabolism. Am J Clin Nutr 83:461S–465S
13. **Strissel KJ, Stancheva Z, Miyoshi H, Perfield 2nd JW, DeFuria J, Jick Z, Greenberg AS, Obin MS** 2007 Adipocyte death, adipose tissue remodeling, and obesity complications. Diabetes 56:2910–2918
14. **Lumeng CN, Bodzin JL, Saltiel AR** 2007 Obesity induces a phenotypic switch in adipose tissue macrophage polarization. J Clin Invest 117:175–184
15. **Rocha VZ, Folco EJ, Sukhova G, Shimizu K, Gotsman I, Vernon AH, Libby P** 2008 Interferon-γ, a Th1 cytokine, regulates fat inflammation. A role for adaptive immunity in obesity. Circ Res 103:467–476
16. **Nguyen MT, Favelyukis S, Nguyen AK, Reichart D, Scott PA, Jenn A, Liu-Bryan R, Glass CK, Neels JG, Olefsky JM** 2007 A subpopulation of macrophages infiltrates hypertrophic adipose tissue and is activated by free fatty acids via Toll-like receptors 2 and 4 and JNK-dependent pathways. J Biol Chem 282:35279–35292
17. **Weisberg SP, McCann D, Desai M, Rosenbaum M, Leibel RL, Ferrante Jr AW** 2003 Obesity is associated with macrophage accumulation in adipose tissue. J Clin Invest 112:1796–1808
18. **Odegaard JI, Chawla A** 2008 Mechanisms of macrophage activation in obesity-induced insulin resistance. Nat Clin Pract 4:619–626
19. **Svec P, Vásárhelyi B, Pászthy B, Körner A, Kovács L, Tulassay T, Treszl A** 2007 Do regulatory T cells contribute to Th1 skewness in obesity? Exp Clin Endocrinol Diabetes 115:439–443
20. **Miller VM, Duckles SP** 2008 Vascular actions of estrogens: functional implications. Pharmacol Rev 60:210–241
21. **Phillips GB, Jing T, Heymsfield SB** 2008 Does insulin resistance, visceral adiposity, or a sex hormone alteration underlie the metabolic syndrome? Studies in women. Metab Clin Exp 57:838–844
22. **Bourgeois F, Alexiu A, Lemonnier D** 1983 Dietary-induced obesity: effect of dietary fats on adipose tissue cellularity in mice. Br J Nutr 49:17–26
23. **Gordon S** 2003 Alternative activation of macrophages. Nat Rev 3:23–35
24. **Murano I, Barbatelli G, Parisani V, Latini C, Muzzonigro G, Castellucci M, Cinti S** 2008 Dead adipocytes, detected as crown-like structures, are prevalent in visceral fat depots of genetically obese mice. J Lipid Res 49:1562–1568
25. **Kolak M, Westerbacka J, Velagapudi VR, Wågsäter D, Yetukuri L, Makkonen J, Rissanen A, Häkkinen AM, Lindell M, Bergholm R, Hamsten A, Eriksson P, Fisher RM, Oresic M, Yki-Järvinen H** 2007 Adipose tissue inflammation and increased ceramide content characterize subjects with high liver fat content independent of obesity. Diabetes 56:1960–1968
26. **Seppälä-Lindroos A, Vehkavaara S, Häkkinen AM, Goto T, Westerbacka J, Sovijärvi A, Halavaara J, Yki-Järvinen H** 2002 Fat accumulation in the liver is associated with defects in insulin suppression of glucose production and serum free fatty acids independent of obesity in normal men. J Clin Endocrinol Metab 87:3023–3028
27. **Isken F, Pfeiffer AF, Nogueiras R, Osterhoff MA, Ristow M, Thorens B, Tschop MH, Weickert MO** 2008 Deficiency of glucose-dependent insulinotropic polypeptide (GIP) receptor prevents ovariectomy-induced obesity in mice. Am J Physiol 295:E350–E355
28. **Ogawa S, Chan J, Gustafsson JA, Korach KS, Pfaff DW** 2003 Estrogen increases locomotor activity in mice through estrogen receptor α: specificity for the type of activity. Endocrinology 144:230–239
29. **Shimomura Y, Shimizu H, Takahashi M, Sato N, Uehara Y, Fukatsu A, Negishi M, Kobayashi I, Kobayashi S** 1990 The significance of decreased ambulatory activity during the generation by long-term observation of obesity in ovariectomized rats. Physiol Behav 47:155–159
30. **Shi H, Kokoeva MV, Inouye K, Tzameli I, Yin H, Flier JS** 2006 TLR4 links innate immunity and fatty acid-induced insulin resistance. J Clin Invest 116:3015–3025
31. **Arkan MC, Hevener AL, Greten FR, Maeda S, Li ZW, Long JM, Wynshaw-Boris A, Poli G, Olefsky J, Karin M** 2005 IKK-β links inflammation to obesity-induced insulin resistance. Nat Med 11:191–198
32. **Perreault M, Marette A** 2001 Targeted disruption of inducible nitric oxide synthase protects against obesity-linked insulin resistance in muscle. Nat Med 7:1138–1143
33. **Patsouris D, Li PP, Thapar D, Chapman J, Olefsky JM, Neels JG** 2008 Ablation of CD11c-positive cells normalizes insulin sensitivity in obese insulin resistant animals. Cell Metab 8:301–309
34. **Juge-Aubry CE, Somm E, Pernin A, Alizadeh N, Giusti V, Dayer JM, Meier CA** 2005 Adipose tissue is a regulated source of interleukin-10. Cytokine 29:270–274
35. **Sowers M, Zheng H, Tomey K, Karvonen-Gutierrez C, Jannausch M, Li X, Yosef M, Symons J** 2007 Changes in body composition in women over six years at midlife: ovarian and chronological aging. J Clin Endocrinol Metab 92:895–901
36. **Weitzmann MN, Pacifici R** 2005 The role of T lymphocytes in bone metabolism. Immunol Rev 208:154–168
37. **Hanley AJ, Williams K, Festa A, Wagenknecht LE, D'Agostino Jr RB, Haffner SM** 2005 Liver markers and development of the metabolic syndrome: the insulin resistance atherosclerosis study. Diabetes 54:3140–3147
38. **Chao L, Marcus-Samuels B, Mason MM, Moitra J, Vinson C, Arioglu E, Gavrilova O, Reitman ML** 2000 Adipose tissue is required for the antidiabetic, but not for the hypolipidemic, effect of thiazolidinediones. J Clin Invest 106:1221–1228
39. **Memon RA, Tecott LH, Nonogaki K, Beigneux A, Moser AH, Grunfeld C, Feingold KR** 2000 Up-regulation of peroxisome proliferator-activated receptors (PPAR-α) and PPAR-γ messenger ribonucleic acid expression in the liver in murine obesity: troglitazone induces expression of PPAR-γ-responsive adipose tissue-specific genes in the liver of obese diabetic mice. Endocrinology 141:4021–4031
40. **Rahimian R, Masih-Khan E, Lo M, van Breemen C, McManus BM, Dubé GP** 2001 Hepatic over-expression of peroxisome proliferator activated receptor γ2 in the ob/ob mouse model of non-insulin dependent diabetes mellitus. Mol Cell Biochem 224:29–37
41. **Bedoucha M, Atzpodien E, Boelsterli UA** 2001 Diabetic KKAy mice exhibit increased hepatic PPARγ1 gene expression and develop hepatic steatosis upon chronic treatment with antidiabetic thiazolidinediones. J Hepatol 35:17–23
42. **Gavrilova O, Haluzik M, Matsusue K, Cutson JJ, Johnson L, Dietz KR, Nicol CJ, Vinson C, Gonzalez FJ, Reitman ML** 2003 Liver peroxisome proliferator-activated receptor γ contributes to hepatic steatosis, triglyceride clearance, and regulation of body fat mass. J Biol Chem 278:34268–34276

43. **Yu S, Matsusue K, Kashireddy P, Cao WQ, Yeldandi V, Yeldandi AV, Rao MS, Gonzalez FJ, Reddy JK** 2003 Adipocyte-specific gene expression and adipogenic steatosis in the mouse liver due to peroxisome proliferator-activated receptor γ1 (PPARγ1) overexpression. J Biol Chem 278:498–505
44. **Schadinger SE, Bucher NL, Schreiber BM, Farmer SR** 2005 PPARγ2 regulates lipogenesis and lipid accumulation in steatotic hepatocytes. Am J Physiol 288: E1195–E1205
45. **Gao H, Bryzgalova G, Hedman E, Khan A, Efendic S, Gustafsson JA, Dahlman-Wright K** 2006 Long-term administration of estradiol decreases expression of hepatic lipogenic genes and improves insulin sensitivity in ob/ob mice: a possible mechanism is through direct regulation of signal transducer and activator of transcription 3. Mol Endocrinol 20:1287–1299
46. **Sahai A, Malladi P, Melin-Aldana H, Green RM, Whitington PF** 2004 Up-regulation of osteopontin expression is involved in the development of non-alcoholic steatohepatitis in a dietary murine model. Am J Physiol Gastrointest Liver Physiol 287:G264–G273
47. **Nomiyama T, Perez-Tilve D, Ogawa D, Gizard F, Zhao Y, Heywood EB, Jones KL, Kawamori R, Cassis LA, Tschop MH, Bruemmer D** 2007 Osteopontin mediates obesity-induced adipose tissue macrophage infiltration and insulin resistance in mice. J Clin Invest 117:2877–2888
48. **Chiba S, Okamoto H, Kon S, Kimura C, Murakami M, Inobe M, Matsui Y, Sugawara T, Shimizu T, Uede T, Kitabatake A** 2002 Development of atherosclerosis in osteopontin transgenic mice. Heart Vessels 16:111–117
49. **Hertrampf T, Schleipen B, Velders M, Laudenbach U, Fritzemeier KH, Diel P** 2008 Estrogen receptor subtype-specific effects on markers of bone homeostasis. Mol Cell Endocrinol 291:104–108